

Article

# Synchrotron Radiation Based Study of the Catalytic Mechanism of $\text{Ag}^+$ to Chalcopyrite Bioleaching by Mesophilic and Thermophilic Cultures

Zhenyuan Nie <sup>1</sup>, Weiwei Zhang <sup>1</sup>, Hongchang Liu <sup>1,2,\*</sup>, Jinlan Xia <sup>1</sup>, Wei Zhu <sup>3</sup>, Duorui Zhang <sup>1</sup>, Lei Zheng <sup>4</sup>, Chenyan Ma <sup>4</sup>, Yidong Zhao <sup>4</sup> and Wen Wen <sup>5</sup>

<sup>1</sup> Key Lab of Biometallurgy of Ministry of Education of China, School of Minerals Processing and Bioengineering, Central South University, Changsha 410083, China; zynie@csu.edu.cn (Z.N.); zhangweiwei@gig.ac.cn (W.Z.); jlxia@csu.edu.cn (J.X.); drzhang@csu.edu.cn (D.Z.)

<sup>2</sup> CAS Key Laboratory of Mineralogy and Metallogeny, Guangzhou Institute of Geochemistry, Chinese Academy of Sciences, Guangzhou 510640, China

<sup>3</sup> College of Science, Hunan University of Technology, Zhuzhou 41000, China; greatcsu@163.com

<sup>4</sup> Beijing Synchrotron Radiation Facility, Institute of High Energy Physics, Chinese Academy of Sciences, Beijing 10049, China; zhenglei@mail.ihep.ac.cn (L.Z.); macny@ihep.ac.cn (C.M.); zhaoyd@ihep.ac.cn (Y.Z.)

<sup>5</sup> Shanghai Synchrotron Radiation Facility, Shanghai Institute of Applied Physics, Chinese Academy of Sciences, Shanghai 201204, China; wenwen@sinap.ac.cn

\* Correspondence: liuhongchang@gig.ac.cn; Tel.: +86-20-85290341

Received: 25 July 2018; Accepted: 31 August 2018; Published: 3 September 2018



**Abstract:** The catalytic mechanism of  $\text{Ag}^+$  for chalcopyrite bioleaching by mesophilic culture (at 30 °C) and thermophilic culture (at 48 °C) was investigated using synchrotron radiation-based X-ray diffraction (SR-XRD) and S K-edge and Fe L-edge X-ray absorption near edge structure (XANES) spectroscopy. Bioleaching experiments showed that copper extraction from chalcopyrite bioleaching by both cultures was promoted significantly by  $\text{Ag}^+$ , with more serious corrosion occurring on the minerals surface. SR-XRD and XANES analyses showed that the intermediates  $\text{S}^0$ , jarosite and secondary minerals (bornite, chalcocite and covellite) formed for all bioleaching experiments. For these secondary minerals, the formation of bornite and covellite was promoted significantly in the presence of  $\text{Ag}^+$  for both cultures, while  $\text{Ag}^+$  has almost no effect on the formation of chalcocite. These results provided insight into the catalytic mechanisms of  $\text{Ag}^+$  to chalcopyrite bioleaching by the mesophilic and thermophilic cultures, which are both probably due to the rapid formation of bornite by  $\text{Ag}^+$  and the conversion of bornite to covellite.

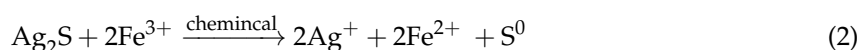
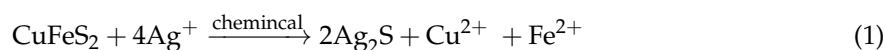
**Keywords:** chalcopyrite; bioleaching;  $\text{Ag}^+$ ; mesophilic culture; thermophilic culture; SR-XRD; XANES

## 1. Introduction

Chalcopyrite is the most abundant copper mineral amongst the copper sulfides and accounts for more than 70% of the copper minerals in the world [1]. In recent decades, due to the excessive consumption of copper concentrate for industrial applications, there is an urgent need to recover copper from low-grade sulfide ores [2,3]. Bioleaching technology is a promising method to recover copper from those ores with advantages such as low-cost and environment-friendly [4]. However, one common problem limiting the application of this technology to industrial applications is that the copper extraction during bioleaching of chalcopyrite is still low [5,6].

To solve this problem, various methods have been investigated to improve the copper extraction rate in chalcopyrite bioleaching, such as adding catalysts ( $\text{Ag}^+$ ,  $\text{Cl}^-$  or carbon materials [7–9]) and

using thermophiles [10]. Among these methods, the addition of  $\text{Ag}^+$  has been proven to be the most effective. Miller and Portillo [11] first reported the improvement for  $\text{Ag}^+$  on chalcopyrite dissolution and proposed a direct reaction model to explain the catalytic mechanism (Equations (1) and (2)). In this model,  $\text{Ag}^+$  first reacts with the chalcopyrite surface  $\text{S}^{2-}$ , forming an  $\text{Ag}_2\text{S}$  crystallite film by exchanging with metal ions; the  $\text{Ag}_2\text{S}$  regenerates  $\text{Ag}^+$  by the oxidation of  $\text{Fe}^{3+}$ ; the released silver ions react with chalcopyrite again. This model also explains that the  $\text{S}^0$  produced in the presence of  $\text{Ag}^+$  is more porous, so that it cannot hinder chalcopyrite dissolution. Parker et al. [12] detected a several hundred nm thick  $\text{Ag}_2\text{S}$  layer on the chalcopyrite surface, providing direct evidence for this model. Wang et al. [13] proposed that  $\text{Ag}_2\text{S}$  formed on the surface of chalcopyrite was through the replacement of copper and iron ions by silver ions. Nazari et al. [14] found that even very small-scale amounts of  $\text{Ag}^+$  could react with the sulfur layer of chalcopyrite and dramatically increase the conductivity of the sulfur layer, thus accelerating chalcopyrite leaching kinetics.



However, by considering how to eliminate the passive layer ( $\text{Cu}_{-x}\text{Fe}_{1-y}\text{S}_2$ ) on the chalcopyrite surface, Ghahremaninezhad et al. suggested that  $\text{Ag}^+$  combined with surface sulfur and then  $\text{Ag}_2\text{S}$  formed and released into solution by taking copper and iron vacancy positions forming the porous sulfur-based product on chalcopyrite surface, so  $\text{Ag}^+$  could continue to catalyze chalcopyrite dissolution by entering the sulfur vacancy [15]. In addition, Wang et al. [8] and Zhao et al. [16] proposed that the addition of  $\text{Ag}^+$  could increase the electrical conductivity of chalcopyrite passive layer.

According to above models,  $\text{Ag}^+$  can interact rapidly with the passive layers (sulfur or  $\text{Cu}_{-x}\text{Fe}_{1-y}\text{S}_2$ ) but the elimination of passive layer probably is not the only reason accelerating dissolution of chalcopyrite in the presence of  $\text{Ag}^+$ , because the surface reactions and the formation of leaching intermediates are very complex. Most recently, to solve this problem, we studied the leaching intermediates formation during bioleaching of chalcopyrite by the archaeal strain *Acidianus manzaensis* YN-25 (grown at 65 °C) in the presence of  $\text{Ag}^+$  by using synchrotron radiation (SR) based XRD (SR-XRD) and XANES [17], revealing that the rapid formation of bornite mostly contributed to promotion effect of  $\text{Ag}^+$  to chalcopyrite bioleaching. This study also indicates that SR- techniques are useful to illustrate the dissolution mechanism during bioleaching and possible contribution of the catalytic effect of  $\text{Ag}^+$ . However, due to the fact that the evolution of intermediates during bioleaching are mainly affected by the iron- and sulfur- oxidizing capabilities of bioleaching microorganisms (such as growth temperatures) [10,18], it is very interesting if the catalytic mechanisms of  $\text{Ag}^+$  could be affected at different bioleaching conditions. Nevertheless, relevant studies have not been conducted and it deserves further investigation.

In this work, two mixed cultures commonly applied in the bioleaching industry, that is, mixed mesophilic culture (grown at 30 °C) and mixed thermophilic culture (grown at 48 °C) were used to evaluate the catalytic effect of  $\text{Ag}^+$  on the bioleaching process of chalcopyrite. SR-XRD and XANES were performed to reveal the correlations between the formation of intermediates and the catalytic effect of  $\text{Ag}^+$ .

## 2. Materials and Methods

### 2.1. Strain and Culture Medium

The bioleaching cultures used in this work were provided by the School of Minerals Processing and Bioengineering, Central South University, Changsha, China. The mixed mesophilic culture (grown at 30 °C) comprised *Leptospirillum ferrooxidans* ZTS, *Acidithiobacillus thiooxidans* A01 and *Acidithiobacillus ferrooxidans* ATCC 23270. The mixed thermophilic culture (grown at 48 °C) comprised *Leptospirillum ferriphilum* YSK, *Acidithiobacillus caldus* S1 and *Sulfobacillus thermosulfidooxidans* YN22. The basal

medium for cultivation of these cultures consisted of:  $(\text{NH}_4)_2\text{SO}_4$ , 3.0 g/L;  $\text{MgSO}_4 \cdot 7\text{H}_2\text{O}$ , 0.5 g/L;  $\text{K}_2\text{HPO}_4$ , 0.5 g/L; KCl, 0.1 g/L;  $\text{Ca}(\text{NO}_3)_2$ , 0.01 g/L. Additionally, 0.2 g/L of yeast extracts were added to the thermophilic culture.

## 2.2. Mineral Samples

The chalcopyrite ( $\text{CuFeS}_2$ ) and the reference minerals, that is, bornite ( $\text{Cu}_5\text{FeS}_4$ ), chalcocite ( $\text{Cu}_2\text{S}$ ), covellite ( $\text{CuS}$ ) and jarosite ( $\text{KFe}_3(\text{SO}_4)_2(\text{OH})_6$ ) were provided by the School of Minerals Processing and Bioengineering, Central South University, Changsha, China and have been commonly used in our previous studies [7,17]. The mineralogical composition tests (by SR-XRD) indicate that the original chalcopyrite is pure mineral (Figure 1). X-ray fluorescence spectroscopic analysis shows that the original chalcopyrite comprised of (mass fraction, wt %): Cu, 33.48; S, 33.05; Fe, 28.99; O, 1.75; Zn, 0.84; Ba, 0.52; Ca, 0.44; Si, 0.38; Al, 0.18; and Mg, 0.09. The original chalcopyrite was ground to 37–74  $\mu\text{m}$  in size and stored in a  $\text{N}_2$  atmosphere at  $-70^\circ\text{C}$ .

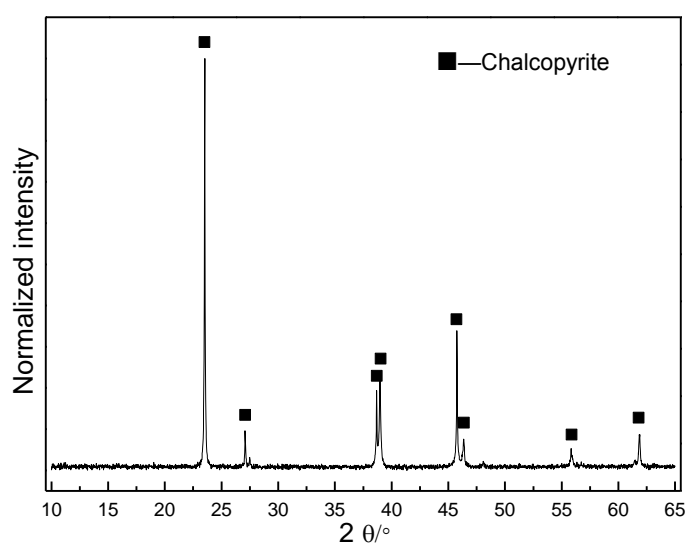


**Figure 1.** Synchrotron radiation-based X-ray diffraction (SR-XRD) patterns of original chalcopyrite.

## 2.3. Bioleaching Experiment

For bioleaching experiments, all cultures were incubated in 500 mL Erlenmeyer flasks containing 2 g chalcopyrite and 200 mL sterilized basal medium, with initial pH 1.8 and inoculated cell density  $4 \times 10^7$  cells/mL. The cultivation of the mixed mesophilic culture and mixed thermophilic culture was performed in rotary shakers (SHZ-GW) at 170 r/min for 28 days, with constant temperatures at  $30^\circ\text{C}$  and  $48^\circ\text{C}$ , respectively. Before experiment, different concentrations of  $\text{Ag}_2\text{SO}_4$  were added to each culture condition. The concentrations of  $\text{Ag}^+$  in solution were presented as 0.1%, 0.2%, 0.3% of the weight of silver to the weight of chalcopyrite, that is, 10, 20 and 30 mg/L, respectively. The bioleaching experiments in the absence of  $\text{Ag}^+$  and the sterile experiment in the presence of 0.1%, 0.2% or 0.3% of  $\text{Ag}^+$  served as controls. The experiments were conducted in triplicate at each condition. During bioleaching, evaporated water was compensated with sterilized ultra-pure water based on weight loss at 24-h and 12-h intervals for the mesophilic culture and thermophilic culture, respectively.

## 2.4. Analytical Methods

### 2.4.1. Leaching Parameters Determination

During bioleaching and sterile control experiments, solutions were taken out at 1 day or 2 days intervals to determine cell densities, pH and redox potential (ORP) values and the concentrations

of  $\text{Cu}^{2+}$  ( $[\text{Cu}^{2+}]$ ),  $\text{Fe}^{3+}$  ( $[\text{Fe}^{3+}]$ ) and total iron ( $[\text{TFe}]$ ) according to previous study [17]. Briefly, cell numbers were counted with an Olympus microscope (BX43). The pH value was determined with a pH meter (PHS-3C). The ORP value was measured with a platinum electrode, using a calomel electrode ( $\text{Hg}/\text{Hg}_2\text{Cl}_2$ ) as reference.  $[\text{Cu}^{2+}]$  was determined using bis-(cyclohexanone)oxalyldihydrazone (BCO) spectrophotometry.  $[\text{Fe}^{3+}]$  and  $[\text{TFe}]$  were determined using 5-sulfosalicylic acid spectrophotometry.  $[\text{Fe}^{3+}]/[\text{TFe}]$  value was calculated based on  $[\text{Fe}^{3+}]$  and  $[\text{TFe}]$ .

#### 2.4.2. Surface Morphology

The surface morphologies were observed using a scanning electron microscopy (SEM) (Nova™ NanoSEM 230, FEI, Hillsboro, OR, USA) as previous study [19].

#### 2.4.3. Chalcopyrite Surface Compositions Analyses

The chalcopyrite surface compositions were analyzed by SR-XRD and XANES spectroscopy. Before these analyses, the solid samples were gently washed three times with diluted sulfuric acid and diluted hydrochloric acid, respectively, to prevent the possible contamination from solution species and dried in vacuum in a vacuum drying oven (DZF-6020, Shaanxi Aoxin Electronic Technology, Shaanxi, China) and stored in nitrogen atmosphere at  $-70\text{ }^\circ\text{C}$ . SR-XRD was detected at BL14B1 beamline of Shanghai Synchrotron Radiation Facility, Shanghai, China, at a step size of  $0.01^\circ$  and a dwell time of 0.5 s with X-ray energy 10 keV and spot size  $0.5 \times 0.5\text{ mm}$ . XANES spectroscopy of S and Fe speciation was performed at 4B7A and 4B7B beamlines of Beijing Synchrotron Radiation Facility, Beijing, China. The S K-edge XANES spectra were scanned between 2460 eV and 2520 eV at step width of 0.2 eV in fluorescence mode at ambient temperature. The Fe L-edge XANES spectra data were recorded from 706 to 728 eV with step size of 0.1 eV in total electron yield mode at ambient temperature. The S K-edge and Fe L-edge XANES spectra were then normalized to the maxima of the absorption spectra and fitted for their linear combinations (LC) using reference spectra with IFEFFIT program according to previous description [20–22].

### 3. Results

#### 3.1. Leaching Characters of Chalcopyrite by Mesophilic Culture in the Presence of $\text{Ag}^+$

During bioleaching by mesophilic culture,  $[\text{Cu}^{2+}]$  of the leaching solution in the presence of 0%, 0.1%, 0.2% and 0.3% of  $\text{Ag}^+$  on day 28 (Figure 2a) was 0.58 g/L ( $\pm 0.0033$ ), 1.54 g/L ( $\pm 0.0093$ ), 2.17 g/L ( $\pm 0.16$ ) and 2.29 g/L ( $\pm 0.19$ ), respectively, corresponding to 17%, 46%, 65% and 68% of Cu extraction, respectively.  $[\text{TFe}]$  of the bioleaching solution in the presence of 0% and 0.1% of  $\text{Ag}^+$  (Figure 2b) increased slowly in the initial stage, increased faster to reach 0.55 g/L ( $\pm 0.0046$ ) on day 26 and 0.96 g/L ( $\pm 0.050$ ) on day 18, respectively and then increased slowly.  $[\text{TFe}]$  in the presence of 0.2% and 0.3% of  $\text{Ag}^+$  (Figure 2b) rapidly reached the greatest value 1.17 g/L ( $\pm 0.044$ ) on day 16 and 1.23 ( $\pm 0.0056$ ) g/L on day 12, respectively and then decreased.

$[\text{Fe}^{3+}]/[\text{TFe}]$  curves for all bioleaching experiments showed similar trends, rapidly increasing to ~100% from day 0 to day 2 and then unchanging (Figure 2c). ORP values of all bioleaching experiments (Figure 2d) increased rapidly to reach 500–550 mV initially and then changed slightly, however, the ORP values of bioleaching experiments in the presence of 0.1–0.3% of  $\text{Ag}^+$  were greater than that without  $\text{Ag}^+$  on days 0–8 but lower on days 16–28.

The pH values for the bioleaching experiment without  $\text{Ag}^+$  (Figure 2e) slowly increased initially, then remained unchanged and then slightly decreased. The pH values for the bioleaching experiment with 0.1% of  $\text{Ag}^+$  (Figure 2e) slowly increased to 1.89 on days 0–8, increased more rapidly to 2.65 on days 8–20 and then changed slightly. While the pH for the bioleaching experiment with 0.2% and 0.3% of  $\text{Ag}^+$  (Figure 2e) increased to 2.17 on day 16 and 2.26 on day 12, respectively and then slowly decreased to 2.10 on day 18 and 2.19 on day 20, respectively and then increased again. The cell densities (Figure 2f) for all bioleaching experiments showed similar trends, increasing to their greatest values

and then changing slightly, while the values of the cell density for the bioleaching experiments with  $\text{Ag}^+$  was slightly greater than that without  $\text{Ag}^+$  at their stationary growth phases.

In contrast,  $[\text{Cu}^{2+}]$  in all sterile experiments at 30 °C (Figure 2a) slowly increased, up to 0.093–0.095 g/L on day 28, corresponding to ~2.8% copper extraction rate.  $[\text{TFe}]$  in all sterile experiments (Figure 2b) slowly reached ~0.09 g/L on day 28. The percentage values of  $[\text{Fe}^{3+}]$  to  $[\text{TFe}]$  for all sterile experiments were zero (Figure 2c). The ORP values increased to 288 mV on day 2 and then remained unchanged (Figure 2d). The pH values increased to 1.87 on day 4 and then changed slightly (Figure 2e). The pH values increased to 1.87 on day 4 and then changed slightly (Figure 2e).

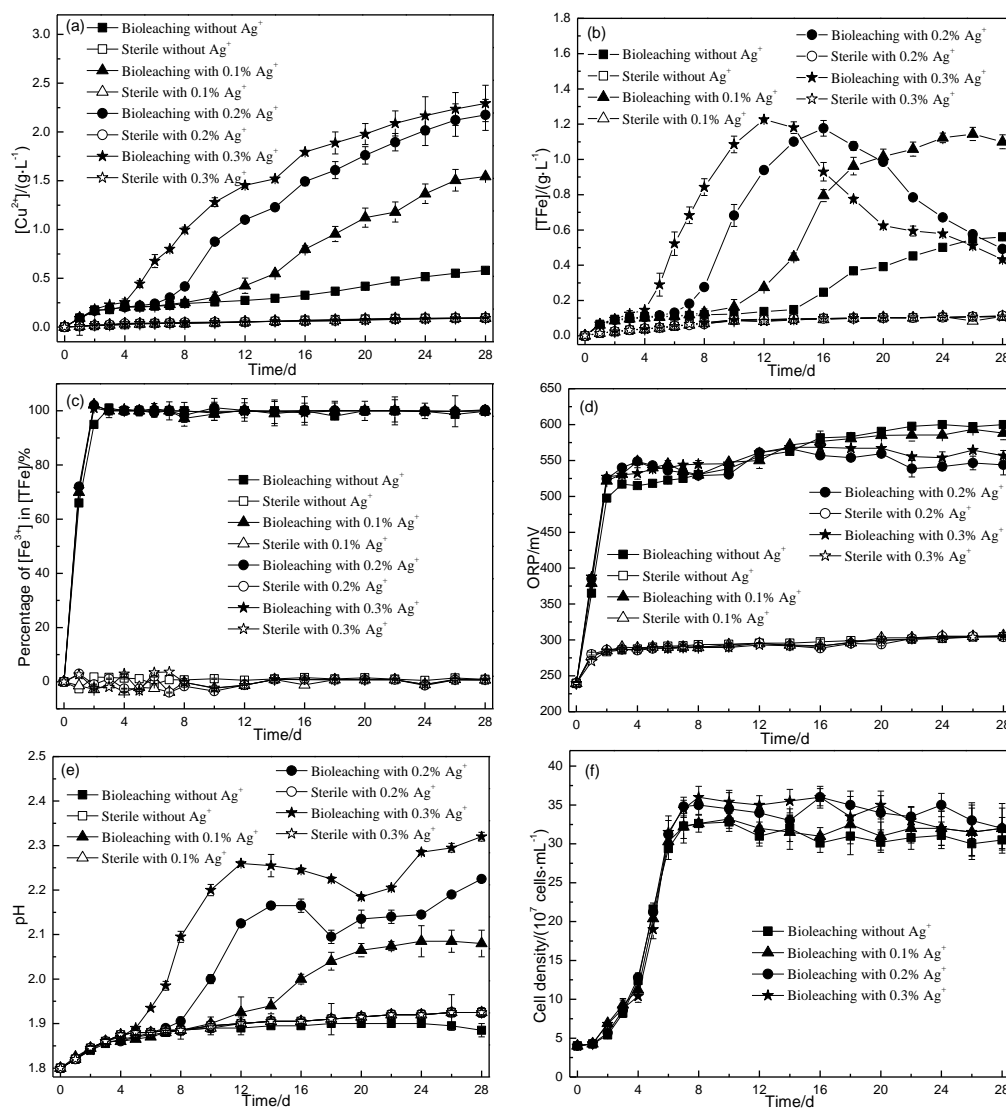


**Figure 2.** Leaching parameters of chalcopyrite by mesophilic culture and in sterile experiments, both at 30 °C with 0, 0.1%, 0.2% and 0.3% of  $\text{Ag}^+$ . The leaching parameters were characterized by  $[\text{Cu}^{2+}]$  (a),  $[\text{TFe}]$  (b), percentages of  $[\text{Fe}^{3+}]/[\text{TFe}]$  (c), ORP values (d), pH values (e) and cell density (f).

### 3.2. Leaching Characters of Chalcopyrite by Thermophilic Culture in the Presence of $\text{Ag}^+$

After 28 d of bioleaching by thermophilic culture,  $[\text{Cu}^{2+}]$  in the presence of 0%, 0.1%, 0.2% and 0.3% of  $\text{Ag}^+$  (Figure 3a) was 1.20 g/L ( $\pm 0.015$ ), 2.95 g/L ( $\pm 0.13$ ), 3.09 g/L ( $\pm 0.097$ ) and 3.16 g/L ( $\pm 0.086$ ), respectively, corresponding to 36%, 88%, 92% and 94% of Cu extraction, respectively.  $[\text{TFe}]$  of the bioleaching solution in the presence of 0.1–0.3% of  $\text{Ag}^+$  (Figure 3b) showed similar trends, rapidly increasing to the greatest values (~0.9 g/L) on day 4–6, then rapidly decreasing and finally changing

slightly. [TFe] for bioleaching without  $\text{Ag}^+$  (Figure 3b) gradually increased to the greatest values on day 20 and then decreased.

The percentage of  $[\text{Fe}^{3+}]$  to [TFe], ORP and cell densities for all bioleaching experiments by thermophilic culture (Figure 3c–f) showed similar trends to that by mesophilic culture (Figure 2c–f), rapidly increasing to the greatest values and then keeping steady. The pH values in the thermophilic and mesophilic systems were different. For bioleaching by thermophilic culture, the pH values in the presence of 0.2–0.3% of  $\text{Ag}^+$  (Figure 3e) increased slightly to pH 1.93–1.95 on day 4, decreased to pH 1.79–1.83 on day 6, increased to the highest pH values (2.35–2.47) on days 14–16 and then decreased. The pH values for the bioleaching experiments with 0.1% of  $\text{Ag}^+$  (Figure 3e) showed similar trends to that with 0.2–0.3% of  $\text{Ag}^+$  but the greatest value was only ~2. The pH values for the bioleaching experiments without  $\text{Ag}^+$  (Figure 3e) changed slightly until day 14 and then gradually decreased.

In contrast, the leaching parameters in all sterile experiments at 48 °C (Figure 3a) showed similar trends to that at 30 °C (Figure 2a), except that the  $[\text{Cu}^{2+}]$  (0.17–0.20 g/L), [TFe] (0.18–0.19 g/L) and ORP (328–334 mV) of the former on day 28 were slightly greater than the latter (with 0.093~0.095 g/L of  $[\text{Cu}^{2+}]$ , 0.11 g/L of [TFe] and ORP 304–306 mV).

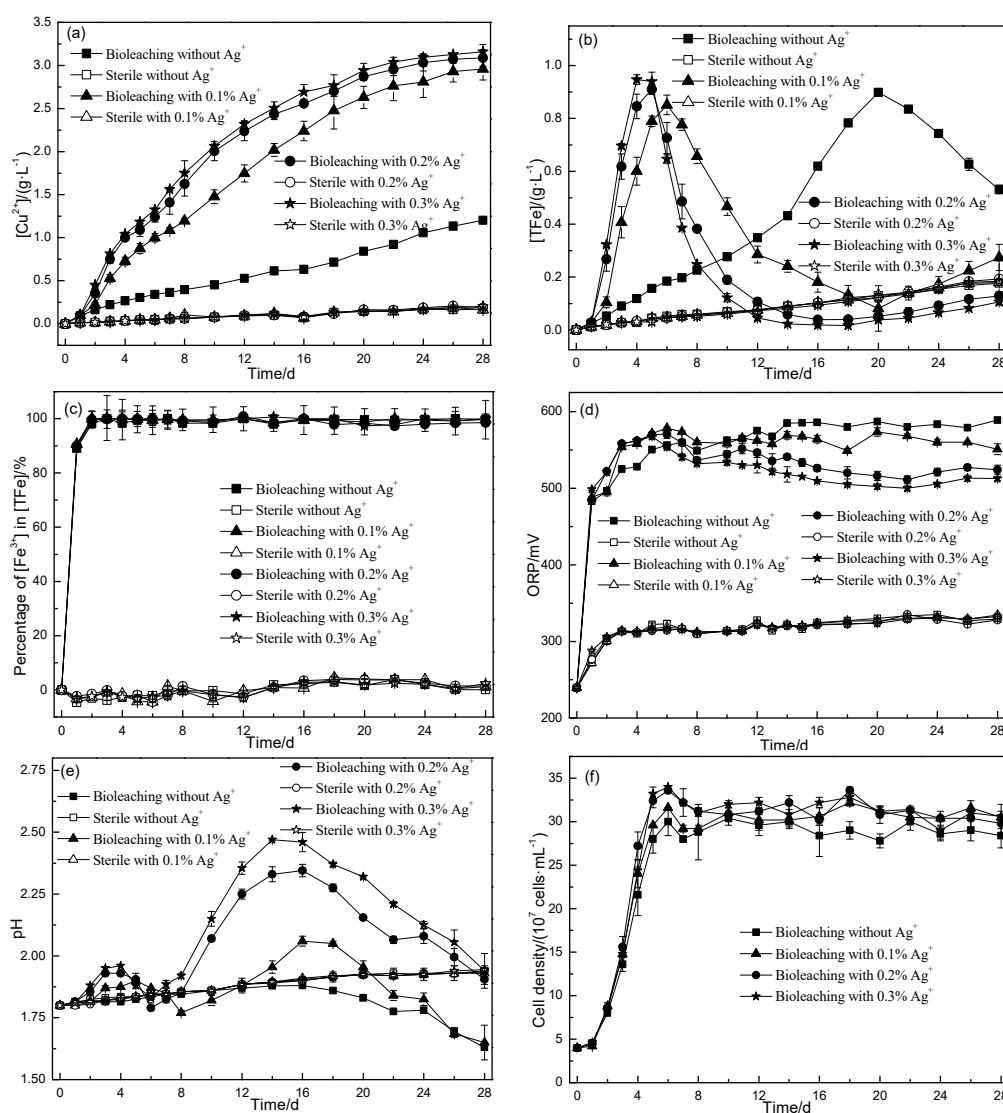


**Figure 3.** Leaching parameters of chalcopyrite by thermophilic culture and in sterile experiments, both at 48 °C with 0, 0.1%, 0.2% and 0.3% of  $\text{Ag}^+$ . The leaching parameters were characterized by  $[\text{Cu}^{2+}]$  (a), [TFe] (b), percentages of  $[\text{Fe}^{3+}]/[\text{TFe}]$  (c), ORP values (d), pH values (e) and cell density (f).

### 3.3. Surface Morphologies of Leaching Residues

The surface of chalcopyrite in the sterile experiments at 30 °C and 48 °C remained unchanged by comparing with original chalcopyrite (Figure 4a).

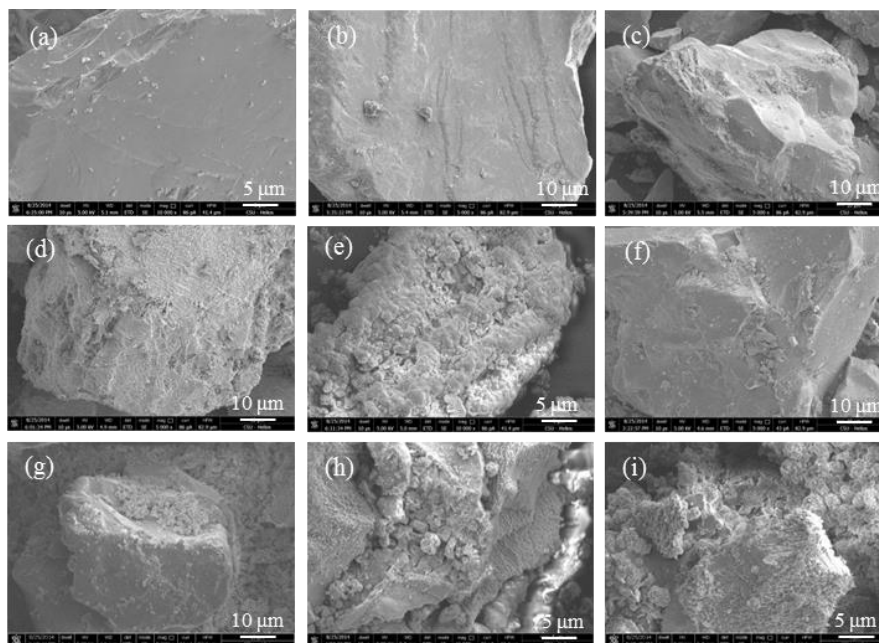


**Figure 4.** Scanning electron microscopy (SEM) micrographs of original chalcopyrite (a) and chalcopyrite bioleached by mesophilic culture without  $\text{Ag}^+$  on day 12 (b) and day 28 (c) and in the presence of 0.3%  $\text{Ag}^+$  on day 12 (d) and day 28 (e); SEM micrographs of chalcopyrite bioleached by thermophilic culture without  $\text{Ag}^+$  on day 12 (f) and day 28 (g) and in the presence of 0.3%  $\text{Ag}^+$  on day 12 (h) and day 28 (i).

The corrosion of chalcopyrite in the presence of mesophilic culture but absence of  $\text{Ag}^+$  was slight, only some granules precipitated on the mineral surface on day 12 (Figure 4b) and day 28 (Figure 4c), while the surfaces of chalcopyrite in the presence of 0.3% of  $\text{Ag}^+$  suffered from serious corrosion, with many etch pits spreading on the surface on day 12 (Figure 4d) and structured granules and porous residues forming on day 28 (Figure 4e).

The surface morphologies of chalcopyrite during bioleached in the presence of thermophilic culture without  $\text{Ag}^+$  (Figure 4f–g) and with  $\text{Ag}^+$  (Figure 4h–i) showed more serious corrosion than that by mesophilic culture, especially for that by thermophilic culture with 0.3% of  $\text{Ag}^+$  (Figure 4i), the size of the residues became smaller and the surface contained more serious etch pits on its surface. The residues were loose combined on the surface of chalcopyrite or fallen off from the mineral particles.

### 3.4. SR-XRD Analysis

The leach residues on day 28 were analyzed using SR-XRD, as shown in Figure 5. For all sterile experiments at 30 °C and 48 °C without  $\text{Ag}^+$  and with 0.3% of  $\text{Ag}^+$ , only little  $\text{S}^0$  and jarosite formed. After bioleaching, the XRD patterns became more complex. For the residues after bioleaching by mesophilic culture and thermophilic culture in the absence of  $\text{Ag}^+$ , the diffraction signal of jarosite and  $\text{S}^0$  were detected, while for bioleaching by both cultures in the presence of 0.3% of  $\text{Ag}^+$ , jarosite,  $\text{S}^0$  and covellite were detected. It should be noted that, for the bioleaching experiments by both cultures with 0.3% of  $\text{Ag}^+$ , only a little chalcopyrite phase was left while jarosite and  $\text{S}^0$  were as the main phases, suggesting that the chalcopyrite dissolution was significantly promoted by  $\text{Ag}^+$  added for both mesophilic culture and thermophilic culture and this result was consistent with the results of  $[\text{Cu}^{2+}]$  curves (Figures 2a and 3a).

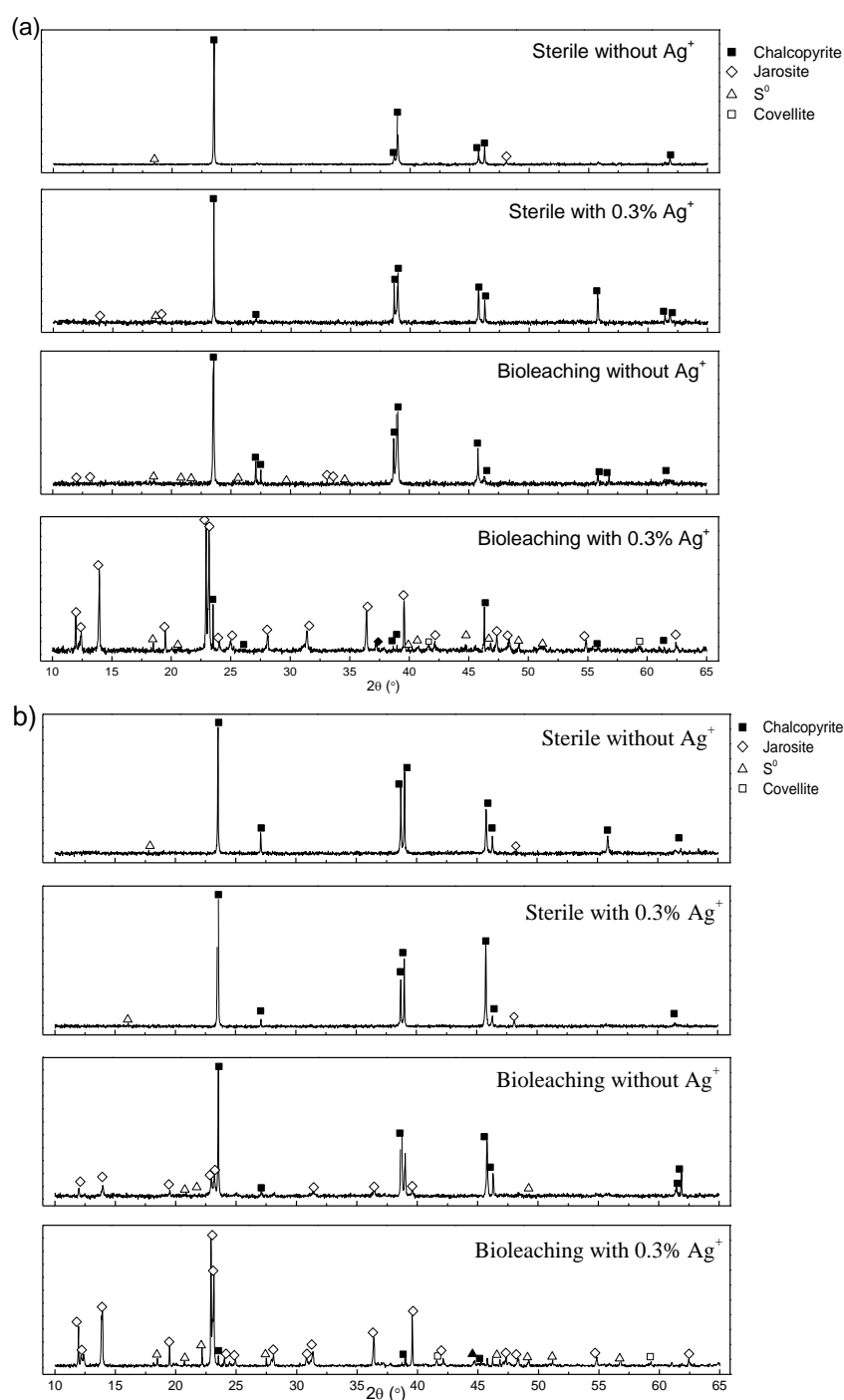


**Figure 5.** SR-XRD patterns of leaching residues by mesophilic culture and in sterile control at 30 °C without  $\text{Ag}^+$  and with 0.3% of  $\text{Ag}^+$  (a) and SR-XRD patterns of leaching residues by thermophilic culture and in sterile control at 48 °C without  $\text{Ag}^+$  and with 0.3% of  $\text{Ag}^+$  (b).

### 3.5. Fe L-Edge and S K-Edge XANES

The Fe and S speciation compositions due to bioleaching by both cultures in the presence of 0.3%  $\text{Ag}^+$  and in the absence of  $\text{Ag}^+$  were analyzed using Fe L-edge and S K-edge XANES spectroscopy, respectively. Results are shown in Figures 6–8.

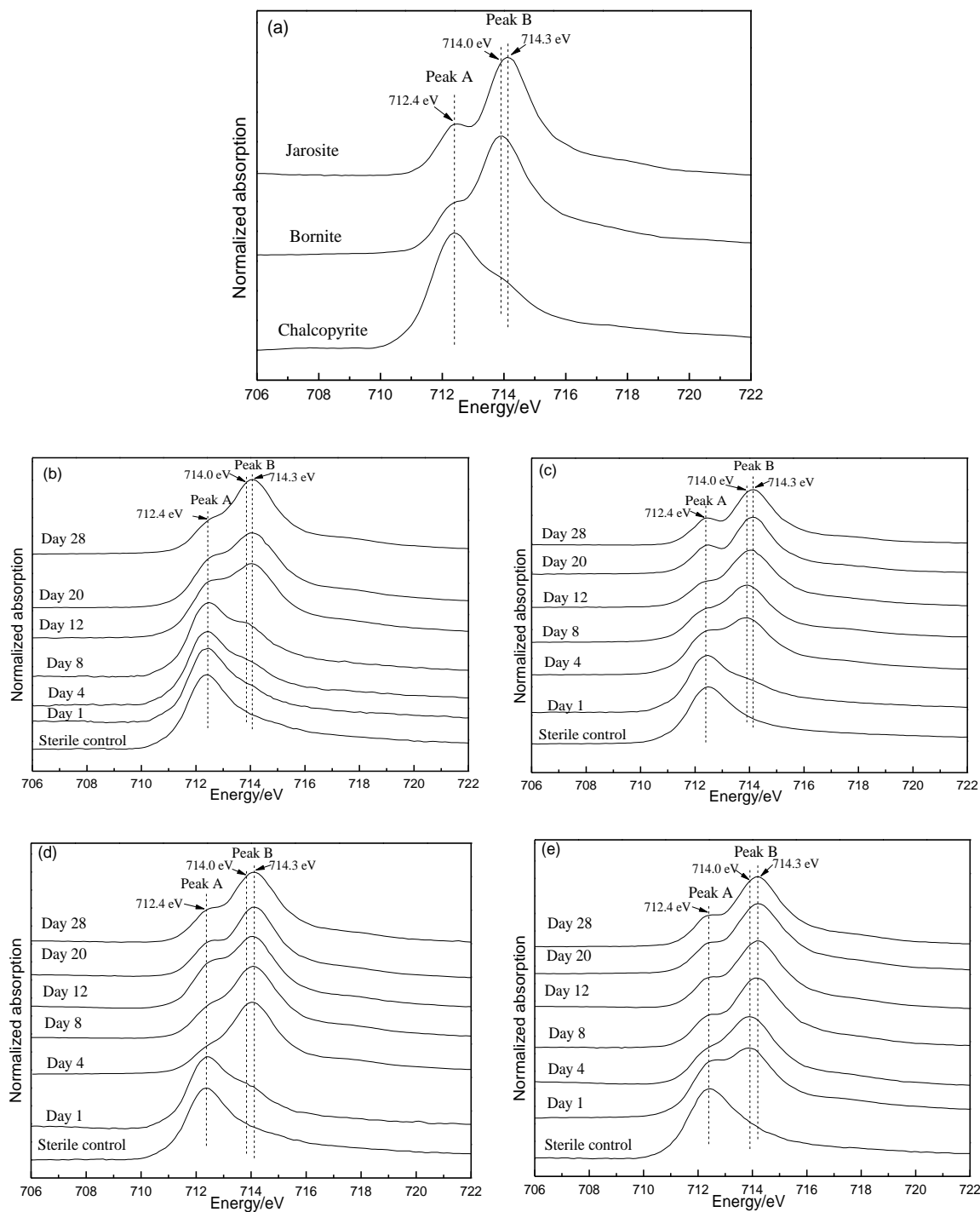


**Figure 6.** Normalized Fe L-edge X-ray absorption near edge structure (XANES) spectra of reference iron-containing compounds (a), chalcopyrite bioleached by mesophilic culture from day 1 to day 28 and in the sterile control at 30 °C on day 28 without  $\text{Ag}^+$  (b) and with 0.3% of  $\text{Ag}^+$  (c) and the spectra of chalcopyrite bioleached by thermophilic culture from day 1 to day 28 and in the sterile control at 48 °C on day 28 without  $\text{Ag}^+$  (d) and with 0.3% of  $\text{Ag}^+$  (e).

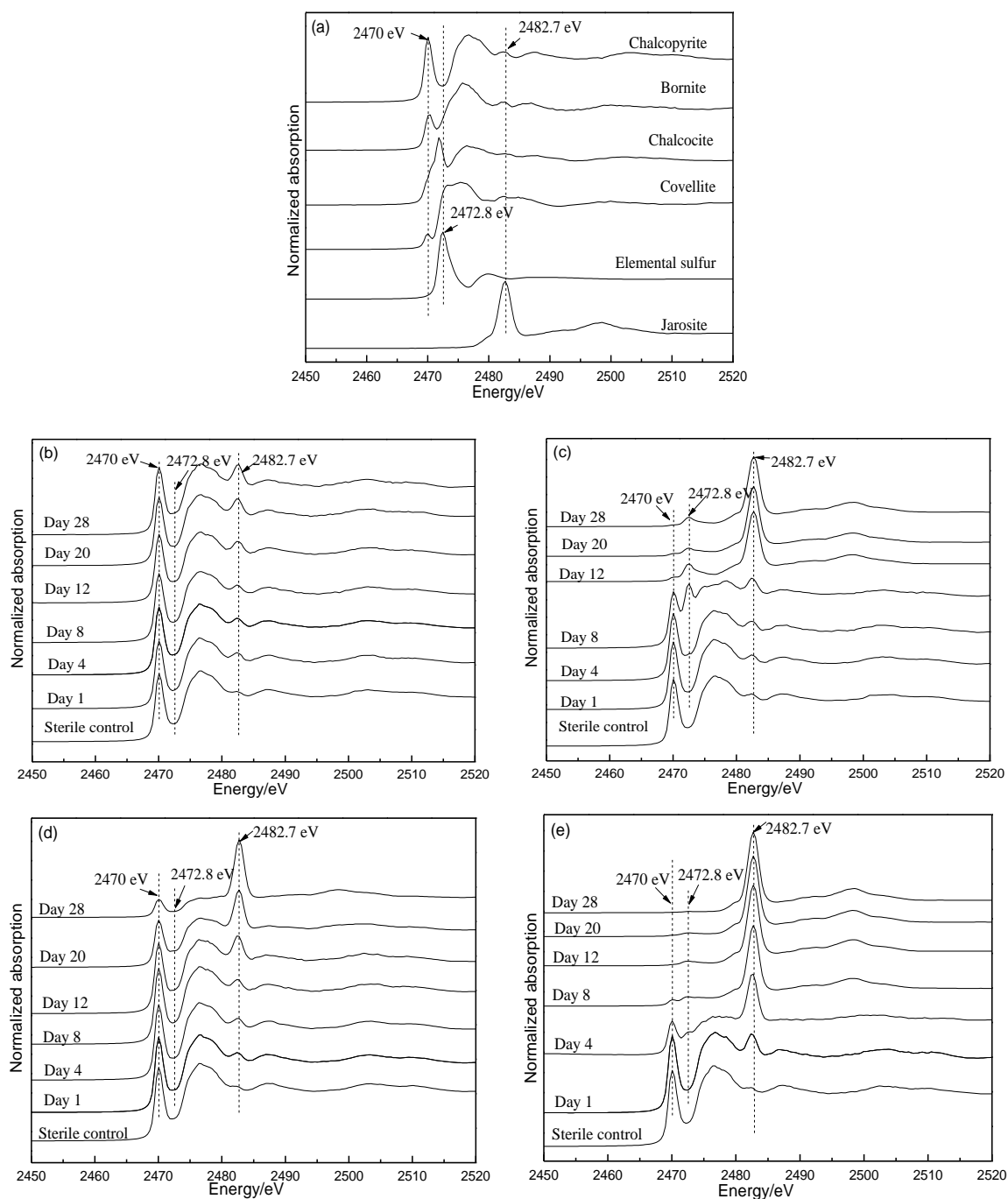


**Figure 7.** Normalized S K-edge XANES spectra of reference sulfur-containing compounds (a), chalcopyrite bioleached by mesophilic culture from day 1 to day 28 and in the sterile control at 30 °C on day 28 without Ag<sup>+</sup> (b) and with 0.3% of Ag<sup>+</sup> (c) and the spectra of chalcopyrite bioleached by thermophilic culture from day 1 to day 28 and in the sterile control at 48 °C on day 28 without Ag<sup>+</sup> (d) and with 0.3% of Ag<sup>+</sup> (e).

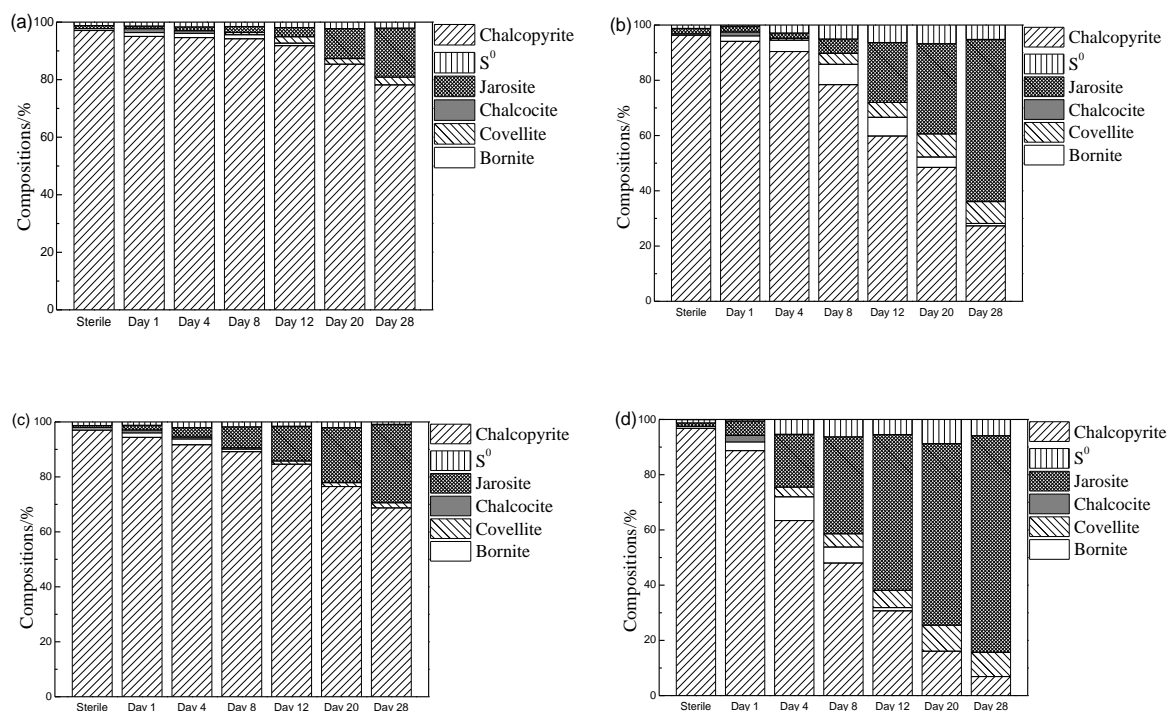


**Figure 8.** Sulfur speciation compositions during chalcopyrite bioleaching by mesophilic culture and in the sterile control at 30 °C without Ag<sup>+</sup> (a) and with 0.3% of Ag<sup>+</sup> (b), and the compositions during chalcopyrite bioleaching by thermophilic culture and in the sterile control at 48 °C without Ag<sup>+</sup> (c) and with 0.3% of Ag<sup>+</sup> (d), by the LC fitting of the unknown spectra from Figure 7b–e with the reference spectra from Figure 7a.

For Fe L-edge XANES analyses, the spectra of reference samples chalcopyrite, bornite and jarosite showed clear differences in their relative intensities of peaks A and B and in their peak positions of peak B (Figure 6a). For the Fe L-edge XANES spectrum of chalcopyrite, the intensity of peak A was greater than that of peak B, while for bornite and jarosite, it was the opposite. For the Fe L-edge XANES spectra of bornite and jarosite, the position of peak B of the former was 0.3 eV less than the latter. It can be seen from Figure 6b–e that the Fe L-edge XANES spectra of leach residues in all the sterile experiments changed slightly. However, for the Fe L-edge XANES spectra of all bioleaching residues, the intensity of peak B gradually increased and became larger than that of peak A after 12 days, 4 days, 4 days and 1 day of bioleaching by mesophilic culture without Ag<sup>+</sup>, mesophilic culture with 0.3% of Ag<sup>+</sup>, thermophilic culture without Ag<sup>+</sup> and thermophilic culture with 0.3% of Ag<sup>+</sup>, respectively. This indicates that the dissolution of chalcopyrite was promoted by Ag<sup>+</sup> added to both cultures and it also indicated that the dissolution of chalcopyrite by thermophilic culture was greater than that by mesophilic culture whether in the presence of Ag<sup>+</sup> or not. It was of particular interest that the peak at 714.0 eV was observed in the spectra of chalcopyrite bioleached by mesophilic culture with Ag<sup>+</sup> on days 4–12 and in the spectra of chalcopyrite bioleached by thermophilic culture with Ag<sup>+</sup> on days 1–4, indicating the iron deficient secondary mineral bornite-like species formed.

For S K-edge XANES analyses, the spectra of the reference samples chalcopyrite, bornite, chalcocite, covellite, S<sup>0</sup> and jarosite showed significant difference in their peaks positions and intensities at 2470, 2472 and 2482.7 eV (Figure 7a). For all sterile experiments, the S K-edge XANES spectra changed slightly on comparison to the original chalcopyrite (Figure 7b–e). For bioleaching by mesophilic culture in the absence of Ag<sup>+</sup> (Figure 7b), the intensity of the peak at 2470 eV remained unchanged and the intensity of the peak at 2482.7 eV increased a little. With 0.3% of Ag<sup>+</sup> (Figure 7c), the intensity of the peak at 2470.0 eV significantly decreased, the intensity of the peak at 2482.7 eV significantly increased and a new peak at 2472.8 eV appeared from day 4. For bioleaching experiments

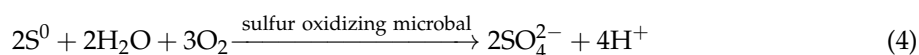
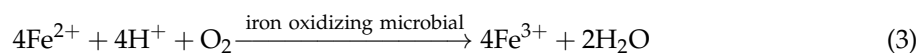
by thermophilic culture in the absence of  $\text{Ag}^+$  (Figure 7d), the peak at 2470 eV gradually decreased and the peak at 2482.7 eV gradually increased. With  $\text{Ag}^+$  (Figure 7e), similar trends were observed to the mesophilic culture with  $\text{Ag}^+$ .

The LC fitting results (Figure 8) of S K-edge XANES spectra in Figure 7b–e with the reference spectra in Figure 7a showed that, after 28 days of bioleaching, the content of chalcopyrite species decreased to 78%, 27%, 69% and 7% for the bioleaching experiments by mesophilic culture without  $\text{Ag}^+$ , mesophilic culture with 0.3% of  $\text{Ag}^+$ , thermophilic culture without  $\text{Ag}^+$  and thermophilic culture with 0.3% of  $\text{Ag}^+$ , respectively. Results also showed that the new  $\text{S}^0$ , jarosite, chalcocite, covellite and bornite species detected during all bioleaching experiments. The contents of bornite and covellite species, as well as  $\text{S}^0$  species for the bioleaching in the presence of both cultures with 0.3% of  $\text{Ag}^+$  (Figure 8b,d) were significantly greater than without  $\text{Ag}^+$  (Figure 8a,c).

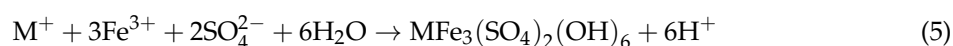
#### 4. Discussion

The bioleaching experiments showed that  $\text{Ag}^+$  significantly promotes the dissolution of chalcopyrite by both mesophilic and thermophilic cultures. For both cultures, within the tested concentrations of  $\text{Ag}^+$  (0.1–0.3%), the greater the concentration of  $\text{Ag}^+$  added, the greater the copper extraction obtained. When 0.3% of  $\text{Ag}^+$  was added, the copper extraction after 28 d of bioleaching increased from 17% to 68% by mesophilic culture (Figure 2a) and from 36% to 94% by thermophilic culture (Figure 3a). It was also confirmed that dissolution of chalcopyrite was more significantly promoted by the thermophilic culture than by mesophilic culture, with greater copper leaching, which was consistent with previous publication [10,17].

According to Equations (1) and (2), the catalytic effect of  $\text{Ag}^+$  on chalcopyrite dissolution would result in greater  $\text{Fe}^{2+}$  and  $\text{S}^0$ . The released  $\text{Fe}^{2+}$  and  $\text{S}^0$  could be further oxidized by bioleaching cultures, because of their iron and sulfur-oxidizing capabilities (Equations (3) and (4)) [23], resulting in  $[\text{TFe}]$ ,  $[\text{Fe}^{3+}]/[\text{TFe}]$ , pH, ORP and cell density in the bioleaching solutions (Figure 2b–f, Figure 3b–f). It should be noted that the curves of each leaching parameter showed a similar trend during bioleaching if the degree of the parameter change is ignored, indicating the addition of  $\text{Ag}^+$  did not change the bacterial sulfur/iron-oxidizing capability of the mesophilic and thermophilic cultures. The effect of  $\text{Ag}^+$  on chalcopyrite bioleaching by the mesophilic and thermophilic cultures in the present study is significantly different with that by the extremely thermophilic archaeal strain *A. manzaensis* [17]. According to Xia et al. [17], the presence of 0.02%–0.1%  $\text{Ag}^+$  could significantly promote copper extraction from chalcopyrite bioleaching by *A. manzaensis* and the optimal concentration of catalyst  $[\text{Ag}^+]$  was 0.05%. No more promotion occurred when  $[\text{Ag}^+]$  was higher than 0.1%; when  $[\text{Ag}^+]$  was  $> 0.05\%$ , the iron-oxidizing capability of the archaeal cells decreased significantly [17]. These differences were probably caused by the cellular structures and resistant capacity to  $\text{Ag}^+$  between bacterial and archaeal cells [24].



With increasing  $[\text{TFe}]$  (mainly  $[\text{Fe}^{3+}]$ ), the pH value increased (Equation 3), resulting in the formation of jarosite (Equation (5)), which was also accelerated by  $\text{Ag}^+$  added for both mesophilic and thermophilic cultures. Some researchers suggested that the formation of jarosite could hinder chalcopyrite dissolution [25,26] but that is still uncertain [27]. The present study showed that jarosite rapidly formed on day 12 and day 4 for bioleaching experiments by the mesophilic and thermophilic cultures, respectively and gradually became a major phase. During the rapid formation of jarosite, chalcopyrite still dissolved rapidly, suggesting jarosite probably not hinder copper extraction for both cultures with and without  $\text{Ag}^+$ .



The  $M^+$  represent a monovalent cation or group, such as  $K^+$ ,  $Na^+$ ,  $H_3O^+$  and  $NH_4^+$ .

Other intermediates formed during bioleaching were  $S^0$  and secondary minerals, bornite, chalcocite and covellite (Figures 5–8). Among these intermediates,  $S^0$  species have also been proposed as one major intermediate hindering chalcopyrite dissolution [28], however it is still controversial [29]. Though microbes with sulfur-oxidizing capability could utilize  $S^0$  as an energy source,  $S^0$  could be continually formed and accumulated on chalcopyrite surface as a thin film associating with other intermediates, suggesting that it is inefficiently utilized by sulfur-oxidizing microorganisms. Some methods have been proposed to eliminate the  $S^0$  layers, for example, adding surfactant [30]. However, in the present study, the greater the amount of  $S^0$  formed during the bioleaching experiment by both mesophilic and thermophilic cultures with 0.3% of  $Ag^+$  did not hinder chalcopyrite dissolution in comparison to leaching without  $Ag^+$ . Miller and Portillo [11] suggested that the presence of  $Ag^+$  could prevent the formation of an impervious  $S^0$  layers on the chalcopyrite surface and instead a porous sulfur film. In the present study, it was also confirmed by surface morphologies of chalcopyrite residues after bioleaching by both mesophilic and thermophilic cultures with  $Ag^+$ , which was looser than that of without  $Ag^+$  (Figure 4), which were also in accordance with Liu et al. [17].

For bioleaching of chalcopyrite, the metal-deficient secondary minerals, such as bornite, chalcocite and covellite, were formed mainly due to the preferential dissolution of Fe. The present study showed that more bornite like species formed for bioleaching experiments by both mesophilic and thermophilic cultures in the presence of  $Ag^+$  (Figure 6, Figure 8). From the results of LC fitting, on days 4–8 for the mesophilic culture and on days 8–12 for the thermophilic culture, bornite was 5~6 times greater than that without  $Ag^+$  (Figure 8). Meanwhile, the copper extraction rate during this period was almost the highest for the bioleaching experiment with  $Ag^+$  by comparison with the other bioleaching experiments. According to previous study [31], bornite is easier to dissolve than chalcopyrite. The formation of bornite like species has been speculated to be a key reason for the accelerated dissolution of chalcopyrite during bioleaching at greater pH (>2.00) and smaller solution ORP (<450 mV) [32] and the formation of bornite during bioleaching by the archaeal strain in the presence of  $Ag^+$  has been proposed to contribute the acceleration of chalcopyrite dissolution at 65 °C [17]. In the present study, it was also found that bornite species could be formed even at a greater ORP (~550 mV), suggesting that the addition of  $Ag^+$  could promote the release of iron and the formation of bornite like species in the presence of the mesophilic and thermophilic cultures with  $Ag^+$ .

It should be noted that, in a proposed model for chalcopyrite dissolution, chalcocite and bornite were formed initially and then gradually transformed to covellite [33–35]. In the present study, we also found that the chalcocite and bornite species formed at the early stage (Figure 8) and then transformed to covellite for both mesophilic and thermophilic cultures in the absence of  $Ag^+$ . After adding  $Ag^+$ , the chalcocite species was found to be no different to that in the absence of  $Ag^+$ , while the covellite species was found ~6 times greater than that in the absence of  $Ag^+$ , suggesting that covellite was probably mainly transformed from bornite under current conditions. On the other hand, according to Yang et al. [36], the accumulation of covellite at the end of chalcopyrite bioleaching could slow down copper extraction. In the present study, we also found the copper extraction was increased slowly on days 20–28, meanwhile covellite was rapidly accumulated, suggesting that covellite like species probably contributes the passivation of chalcopyrite in the presence of the mesophilic and thermophilic cultures. Thus, it can be speculated that the rapid dissolution of chalcopyrite by both mesophilic and thermophilic cultures in the presence of catalyst  $Ag^+$  is also probably due to the rapid transformation of chalcopyrite to bornite and the conversion of bornite to covellite, however, the accumulation of covellite could be a key reason that copper dissolution slowing down at the late stage of the bioleaching. In addition, it is also indicated that the rapid formation of bornite and the conversion of bornite to covellite for the bioleaching of chalcopyrite in the presence of  $Ag^+$  is not at all affected by types of bioleaching cultures and their growth temperatures.

## 5. Conclusions

Bioleaching experiment has shown that  $\text{Ag}^+$  can significantly promote the dissolution of chalcopyrite by both mesophilic and thermophilic cultures. In addition, the dissolution of chalcopyrite can be more significantly promoted by the thermophilic culture than that by the mesophilic culture, with more serious corrosion on the mineral surfaces. XRD and XANES analyses showed that the leaching intermediates  $\text{S}^0$ , jarosite and secondary minerals bornite, chalcocite and covellite formed during all bioleaching experiments. The formation of  $\text{S}^0$  or jarosite on chalcopyrite bioleaching probably had no negative effect on chalcopyrite bioleaching in the presence of  $\text{Ag}^+$ . For the bioleaching experiments by both mesophilic and thermophilic cultures, the formation of bornite and covellite was distinctly promoted by addition of  $\text{Ag}^+$ , providing insight that the catalytic mechanism of  $\text{Ag}^+$  with regard to chalcopyrite bioleaching by mesophilic culture and thermophilic culture is probably by promoting the rapid formation of bornite and the conversion of bornite to covellite.

**Author Contributions:** Z.N., H.L. and J.X. conceived and designed the experiments; Z.N., W.Z., H.L., D.Z. and W.Z. performed the experiments; Z.N., W.Z. and H.L. analyzed the data; L.Z., C.M. and Y.Z. contributed reagents/materials/analysis tools; Z.N., H.L. and J.X. wrote the paper.

**Funding:** This research was funded by National Natural Science Foundation of China [41802038, U1608254, 51774342, 51404104], Natural Science Foundation of Guangdong Province (2017A030313219), National Postdoctoral Program for Innovative Talents (BX201600165), China Postdoctoral Science Foundation (2016M600688) and Open Funds of Bingjing Synchrotron Radiation Facility (2017-BEPC-PT-001052/1065) and Shanghai Synchrotron Radiation Facility (2017-SSRF-PT-002777).

**Acknowledgments:** We thank the staff of Bingjing Synchrotron Radiation Facility and Shanghai Synchrotron Radiation Facility for their help to collect SR-XRD and XANES data. We also thank to the three anonymous reviewers for their constructive review.

**Conflicts of Interest:** The authors declare no conflict of interest.

## References

- Pradhan, N.; Nathsarma, K.C.; Srinivasa, R.K.; Sukla, L.B.; Mishra, B.K. Heap bioleaching of chalcopyrite: A review. *Miner. Eng.* **2008**, *21*, 355–365. [[CrossRef](#)]
- Li, Y.; Kawashima, N.; Li, J.; Chandra, A.P.; Gerson, A.R. A review of the structure and fundamental mechanisms and kinetics of the leaching of chalcopyrite. *Adv. Colloid Interface Sci.* **2013**, *197–198*, 1–32. [[CrossRef](#)] [[PubMed](#)]
- Watling, H.R. The bioleaching of sulphide minerals with emphasis on copper sulphides—A review. *Hydrometallurgy* **2006**, *84*, 81–108. [[CrossRef](#)]
- Dew, D.W.; Van, B.C.; Mcewan, K.; Bowker, C. Bioleaching of base metal sulphide concentrates: A comparison of high and low temperature bioleaching. *J. S. Afr. Inst. Min. Metall.* **2000**, *100*, 409–413.
- Gu, G.; Hu, K.; Zhang, X.; Xiong, X.; Yang, H. The stepwise dissolution of chalcopyrite bioleached by *Leptospirillum ferriphilum*. *Electrochim. Acta* **2013**, *103*, 50–57. [[CrossRef](#)]
- Feng, S.; Yang, H.; Xin, Y.; Gao, K.; Yang, J.; Liu, T.; Zhang, L.; Wang, W. A novel and highly efficient system for chalcopyrite bioleaching by mixed strains of *Acidithiobacillus*. *Bioresour. Technol.* **2013**, *129*, 456–462. [[CrossRef](#)] [[PubMed](#)]
- Liang, C.; Xia, J.; Nie, Z.; Yang, Y.; Ma, C. Effect of sodium chloride on sulfur speciation of chalcopyrite bioleached by the extreme thermophile *Acidianus manzaensis*. *Bioresour. Technol.* **2012**, *110*, 462–467.
- Wang, J.; Liao, R.; Tao, L.; Zhao, H.; Zhai, R.; Qin, W.; Qiu, G. A comprehensive utilization of silver-bearing solid wastes in chalcopyrite bioleaching. *Hydrometallurgy* **2017**, *169*, 152–157. [[CrossRef](#)]
- Hao, X.; Liu, X.; Zhu, P.; Chen, A.; Liu, H.; Yin, H.; Qiu, G.; Liang, Y. Carbon material with high specific surface area improves complex copper ores' bioleaching efficiency by mixed moderate thermophiles. *Minerals* **2018**, *8*, 301. [[CrossRef](#)]
- Liu, H.; Xia, J.; Nie, Z.; Liu, L.; Wang, L.; Ma, C.; Zheng, L.; Zhao, Y.; Wen, W. Comparative study of S, Fe and Cu speciation transformation during chalcopyrite bioleaching by mixed mesophiles and mixed thermophiles. *Miner. Eng.* **2017**, *106*, 22–32. [[CrossRef](#)]

11. Miller, J.D.; Portillo, H.Q. Electrochemistry in silver catalysed ferric sulfate leaching of chalcopyrite. *J. Macromol. Sci.* **1981**, *27*, 327–338.
12. Parker, A.; Klauber, C.; Kougiianos, A.; Watling, H.R.; Van Bronswijk, W. An X-ray photoelectron spectroscopy study of the mechanism of oxidative dissolution of chalcopyrite. *Hydrometallurgy* **2003**, *71*, 265–276. [[CrossRef](#)]
13. Wang, M.; Zhang, Y.; Deng, T.; Wang, K. Kinetic modeling for the bacterial leaching of chalcopyrite catalyzed by silver ions. *Miner. Eng.* **2004**, *17*, 943–947. [[CrossRef](#)]
14. Nazari, G.; Dixon, D.G.; Dreisinger, D.B. The mechanism of chalcopyrite leaching in the presence of silver-enhanced pyrite in the Galvanox™ process. *Hydrometallurgy* **2012**, *113–114*, 122–130. [[CrossRef](#)]
15. Ghahremaninezhad, A.; Radzinski, R.; Gheorghiu, T.; Dixon, D.G.; Asselin, E. A model for silver ion catalysis of chalcopyrite (CuFeS<sub>2</sub>) dissolution. *Hydrometallurgy* **2015**, *155*, 95–104. [[CrossRef](#)]
16. Zhao, H.; Wang, J.; Gan, X.; Hu, M.; Zhang, E.; Qin, W.; Qiu, G. Cooperative bioleaching of chalcopyrite and silver-bearing tailing by mixed moderately thermophilic culture: An emphasis on the chalcopyrite dissolution with XPS and electrochemical analysis. *Miner. Eng.* **2015**, *81*, 23–29. [[CrossRef](#)]
17. Xia, J.; Song, J.; Liu, H.; Nie, Z.; Shen, L.; Yuan, P.; Ma, C.; Zheng, L.; Zhao, Y. Study on catalytic mechanism of silver ions in bioleaching of chalcopyrite by SR–XRD and XANES. *Hydrometallurgy* **2018**, *180*, 26–35. [[CrossRef](#)]
18. Liu, H.; Xia, J.; Nie, Z.; Zhu, H.; Zhao, Y.; Ma, C.; Zheng, L. Evolution of leaching products on the surface of chalcopyrite by mesophiles and thermophiles based on SR–XRD and XANES spectroscopy. *Adv. Mater. Res.* **2015**, *1130*, 183–187. [[CrossRef](#)]
19. Liu, H.; Xia, J.; Nie, Z. Relatedness of Cu and Fe speciation to chalcopyrite bioleaching by *Acidithiobacillus Ferrooxidans*. *Hydrometallurgy* **2015**, *156*, 40–46. [[CrossRef](#)]
20. Ide–Ektessabi, A.; Kawakami, T.; Watt, F. Distribution and chemical state analysis of iron in the Parkinsonian substantia nigra using synchrotron radiation micro beams. *Nucl. Instrum. Methods. B* **2004**, *213*, 590–594. [[CrossRef](#)]
21. Ravel, B.; Newville, M. ATHENA. ARTEMIS, HEPHAESTUS: Data analysis for X-ray absorption spectroscopy using IFEFFIT. *J. Synchrotron Radiat.* **2005**, *12*, 537–541. [[CrossRef](#)] [[PubMed](#)]
22. Prange, A. Speciation analysis of microbiologically produced sulfur by X-ray absorption near edge structure spectroscopy. In *Microbial Sulfur Metabolism*; Dahl, C., Friedrich, C.G., Eds.; Springer: Heidelberg, Germany, 2008; pp. 259–272.
23. Vera, M.; Schippers, A.; Sand, W. Progress in bioleaching: fundamentals and mechanisms of bacterial metal sulfide oxidation—Part A. *Appl. Microbiol. Biotechnol.* **2013**, *97*, 7529–7541. [[CrossRef](#)] [[PubMed](#)]
24. Raheb, J.; Sharoknyan, S.; Nazari, F.; Rakhshany, Y. The studying of silver nanoparticle effect on the copper bioleaching output from low grade sulfidic ores. *Am. J. Nano Res. Appl.* **2015**, *3*, 6–11.
25. Klauber, C. A critical review of the surface chemistry of acidic ferric sulphate dissolution of chalcopyrite with regards to hindered dissolution. *Int. J. Miner. Process.* **2008**, *86*, 1–17. [[CrossRef](#)]
26. Pan, H.; Yang, H.; Tong, L.; Zhong, C.; Zhao, Y. Control method of chalcopyrite passivation in bioleaching. *Trans. Nonferrous Met. Soc. China* **2012**, *22*, 2255–2260. [[CrossRef](#)]
27. Majuste, D.; Ciminelli, V.S.T.; Osseo-Asare, K.; Dantas, M.S.S.; Magalhães-Paniago, R. Electrochemical dissolution of chalcopyrite: Detection of bornite by synchrotron small angle X-ray diffraction and its correlation with the hindered dissolution process. *Hydrometallurgy* **2012**, *111–112*, 114–123. [[CrossRef](#)]
28. Harmer, S.L.; Thomas, J.E.; Fornasiero, D.; Gerson, A.R. The evolution of surface layers formed during chalcopyrite leaching. *Geochim. Cosmochim. Acta* **2006**, *70*, 4392–4402. [[CrossRef](#)]
29. Li, Y.; Qian, G.; Li, J.; Gerson, A.R. Kinetics and roles of solution and surface species of chalcopyrite dissolution at 650 Mv. *Geochim. Cosmochim. Acta* **2015**, *161*, 188–202. [[CrossRef](#)]
30. Peng, A.; Liu, H.; Nie, Z.; Xia, J. Effect of surfactant Tween-80 on sulfur oxidation and expression of sulfur metabolism relevant genes of *Acidithiobacillus ferrooxidans*. *Trans. Nonferrous Met. Soc. China* **2012**, *22*, 3147–3155. [[CrossRef](#)]
31. Zhao, H.; Wang, J.; Gan, X.; Hu, M.; Zhang, E.; Qin, W.; Qiu, G. Comparison of electrochemical dissolution of chalcopyrite and bornite in acid culture medium. *Trans. Nonferrous Met. Soc. China* **2015**, *25*, 303–313. [[CrossRef](#)]
32. Liu, H.; Xia, J.; Nie, Z.; Ma, C.; Zheng, L.; Hong, C.; Zhao, Y.; Wen, W. Bioleaching of chalcopyrite by *Acidianus manzaensis* under different constant pH. *Miner. Eng.* **2016**, *98*, 80–89. [[CrossRef](#)]

33. Hiroyoshi, N.; Tsunekawa, M.; Okamoto, H.; Nakayama, R.; Kuroiwa, S. Improved chalcopryrite leaching through optimization of redox potential. *Can. Metall. Q.* **2008**, *47*, 253–258. [[CrossRef](#)]
34. Hiroyoshi, N.; Arai, M.; Miki, H.; Tsunekawa, M.; Hirajima, T. A new reaction model for the catalytic effect of silver ions on chalcopryrite leaching in sulfuric acid solutions. *Hydrometallurgy* **2002**, *63*, 257–267. [[CrossRef](#)]
35. Liu, H.; Xia, J.; Nie, Z.; Wen, W.; Yang, Y.; Ma, C.; Zheng, L.; Zhao, Y. Formation and evolution of secondary minerals during bioleaching of chalcopryrite by thermoacidophilic Archaea *Acidianus manzaensis*. *Trans. Nonferrous Met. Soc. China* **2016**, *26*, 2485–2494. [[CrossRef](#)]
36. Yang, Y.; Liu, W.; Chen, M. A copper and iron K-edge XANES study on chalcopryrite leached by mesophiles and moderate thermophiles. *Miner. Eng.* **2013**, *48*, 31–35. [[CrossRef](#)]



© 2018 by the authors. Licensee MDPI, Basel, Switzerland. This article is an open access article distributed under the terms and conditions of the Creative Commons Attribution (CC BY) license (<http://creativecommons.org/licenses/by/4.0/>).